

## Research Article

Aditi Ghosh\*, Pradyuta Padmanabhan, Anuj Mubayi, and Padmanabhan Seshaiyer

# Influence of distinct social contexts of long-term care facilities on the dynamics of spread of COVID-19 under predefined epidemiological scenarios

<https://doi.org/10.1515/cmb-2023-0102>

received May 17, 2023; accepted September 7, 2023

**Abstract:** More than half of the coronavirus disease 19 (COVID-19) related mortality rates in the United States and Europe are associated with long-term-care facilities (LTCFs) such as old-age organizations, nursing homes, and disability centers. These facilities are considered most vulnerable to spread of an pandemic like COVID-19 because of multiple reasons including high density of elderly population with a diverse range of medical requirements, limited resources, nursing activities/medications, and the role of external visitors. In this study, we aim to understand the role of visitor's family members and specific interventions (such as use of face masks and restriction of visiting hours) on the dynamics of infection in a community using a mathematical model. The model considers two types of social contexts (community and LTCFs) with three different groups of interacting populations (non-mobile community individuals, mobile community individuals, and long-term facility residents). The goal of this work is to compare the outbreak burden between different centre of disease control (CDC) planning scenarios, which capture distinct types of intensity of diseases spread in LTCF observed during COVID-19 outbreak. The movement of community mobile members is captured via their average relative times in and out of the long-term facilities to understand the strategies that would work well in these facilities the CDC planning scenarios. Our results suggest that heterogeneous mixing worsens epidemic scenario as compared to homogeneous mixing and the epidemic burden is hundreds times greater for community spread than within the facility population.

**Keywords:** COVID19, long-term care, model, infectious disease

**MSC 2020:** 00A71

## 1 Introduction

Ever since the coronavirus disease 19 (COVID-19) pandemic first surfaced in the United States, the number of cases and deaths in nursing homes and other long-term care facilities (LTCFs) has been increasing. In 2020, it is reported that at minimum 28,100 residents and workers passed away from COVID-19 infection at nursing homes and other LTCFs for senior adults in the United States, according to a New York Times database. The

---

\* Corresponding author: Aditi Ghosh, Department of Mathematics, Texas A&M University-Commerce, Monroe St, Commerce, 75402, TX, USA, e-mail: aditi.ghosh@tamuc.edu

Pradyuta Padmanabhan: Department of Mathematics, University of Pittsburgh, Fifth Avenue, Pittsburgh, 15260, Pennsylvania, USA, e-mail: pradyuta@gmail.com

Anuj Mubayi: The Intercollegiate Biomathematics Alliance, Illinois State University, Normal, 61790, Illinois, USA, e-mail: anujmubayi@yahoo.com

Padmanabhan Seshaiyer: Department of Mathematical Sciences, George Mason University, 4400 University Drive, Fairfax, 22030, Virginia, USA, e-mail: pseshaiy@gmu.edu

number of infected cases was more than 153,000 at some 7,700 facilities [30]. In at least six states, senior residents in LTCF accounted for 50% or more of all COVID-19 deaths. New York Times mentioned that 11% of the cases in United States resulted from these facilities. The number of deaths due to COVID-19 in these facilities attributed to more than a third of the country's pandemic fatalities [30]. States varied with known cases in LTCFs, with New Jersey (528) and Pennsylvania (539) topping the list, and New York (430), California (525), Washington (243), Maine (9), Iowa (32), and New Mexico (27), Alabama (5) reporting the lowest number of facilities [15,30]. Highest number of cases over 11,000 cases in LTCFs were reported in New Jersey of all the 29 states, [15]. Lesser than 100 cases were reported from South Dakota and Montana in these facilities [30].

The steady increase in deaths among LTCF residents due to COVID-19 had become an urgent concern for federal and state policymakers, LTCFs, family members of residents, and residents themselves [16]. Many residents and staff members in LTCF identified with COVID-19 were asymptomatic and pre-symptomatic and hence spread the disease very rapidly in the facility. During the period of March 29–April 10 at the Veterans affairs Greater Los Angeles Healthcare System, many residents, staff had positive test results for COVID-19. About 19% residents and 6% staff members tested positive for COVID-19 [18]. In a LTCF in King County, Washington, the hospitalization rates as of March 18 due to COVID-19 were 54.5, 50.0, and 6% for facility residents, visitors, and staff, respectively. The case fatality rate for residents was 33.7% [22]. The findings from [22] indicate that outbreak of COVID-19 in LTCFs had a significant impact on vulnerable older adults with pre-existing health conditions and local health care systems.

While young adults may not be likely to become infected severely by COVID-19 as older adults, there is evidence that the youth and the middle-aged can potentially play an important in preventing the spread of COVID-19, so the most vulnerable can be protected from getting sick. A study in 2020 [2,13,26,27] indicate that the hospitalization rate and death are more closely correlated with older people. The Centers for Medicare and Medicaid Services recently directed all LTCFs to significantly restrict visitors and non-essential personnel, as well as restrict communal activities inside LTCFs. The guidance that is based upon centre of disease control (CDC) recommendations directed LTCFs to restrict visitation except in certain compassionate cases, like end-of-life. In those cases, visitors were equipped with personal protective equipment such as masks, and the visit will be limited to a specific room only.

While such measures were directed a couple of years back, there are, however, still gaps in controls at LTCFs. Given that 1.3 million elderly adults live permanently in about 15,000 LTCFs nationwide with more than half over the age of 75, more coronavirus outbreaks are expected. Visitors and staff going to visit LTCFs may be carrying the virus and transmit to the elderly LTCFs residents who are highly susceptible to the virus. Similarly, those in the resident homes that have the virus have the potential to transfer the disease to the visitors as well. This is the motivation for this work [23,29].

A review of important contributions to the mathematical theory of epidemics can be found in several articles from the pioneering work of Fred Brauer [1,3–7,19]. The Kermack-Mckendrick compartmental model was considered as one of the earliest attempts to formulate a simple mathematical model to predict the spread of an infectious disease where the population being studied is divided into compartments, namely, a susceptible class *S*, an infective class *I*, and a removed class *R*. Building on this simple susceptible-infectious-recovered model, there have been several models that have been developed to address various infectious diseases [8]. Along with these foundational compartmental models to understand disease propagation, models for understanding disease dynamics during mass transportation have also been studied. For example, [11] developed a model to study the smallpox transmission on a widely used mass transportation system, the subway. In this model, the population in each neighborhood is subdivided into subway and non-subway users to understand the disease dynamics and its control in a city. We extend this idea to divide the population in a neighborhood into two groups: one visiting the long-term care center and the other does not to study the COVID-19 spread in the neighborhood.

**Goal of the study:** There are multiple objectives of the study, including: (i) to develop and analyze a mathematical model that will integrate two groups of adult population, one that does not visit LTCFs and the other that visits LTCFs along with a group of older vulnerable residents of a LTCF; (ii) to understand the role of visitors of the residents in LTCFs and specific nonpharmaceutical interventions such as the use of face masks and restriction of visiting hours on the dynamics of infection in a community using the developed model; (iii)

to capture and compare the five standard CDC scenarios to evaluate ongoing non-pharmaceutical interventions; and (iv) to study the role of population mixing assumptions that can capture changes in human behaviors. In order to study these objectives, two types of social contexts (community and LTCFs) are considered in the model along with three different groups of interacting populations (non-mobile community individuals, mobile community individuals that frequents LTCFs, and the residents there).

The rest of this article is divided as follows. Section 2 discusses the model formulation along with the mixing probabilities and basic reproductive number. We also implemented the CDC strategies in Section 2. Numerical results are discussed in Section 3 and conclusion in Section 4.

## 2 Models and background

### 2.1 Model description

In our model, we consider a city where we subdivide the population into three categories: individuals of the community that do not visit LTCF (Q), individuals from the community who visit a long-term care (T), and the LTCF residents (P). We refer to the members of Q and T population to be *non-mobile* and *mobile* individuals, respectively. The third group in our model includes LTCF residents (P) who will be referred to as *senior* members. The members of the sub-population of T are expected to interact with both sub-populations Q and P, respectively. Besides, disease can also be passed on through interaction within each sub-group as well (Figure 1).

Within each of the sub-groups, we use an S-E-I-R type model that denotes the respective susceptible, exposed (asymptomatic), infectious (symptomatic), and recovered. For our model, the Q sub-population is modeled using  $S, E, I$ , and  $R$  to denote the respective epidemiological states with total population  $Q = S + E + I + R$ , the T sub-population model using  $W, X, Y$ , and  $Z$  compartments with total population  $T = W + X + Y + Z$ , and the older long-term facility group P using the compartments  $A, B, C$ , and  $D$  with total population  $P = A + B + C + D$ . Next, we describe the compartmental models for the three sub-populations defined in Table 1.

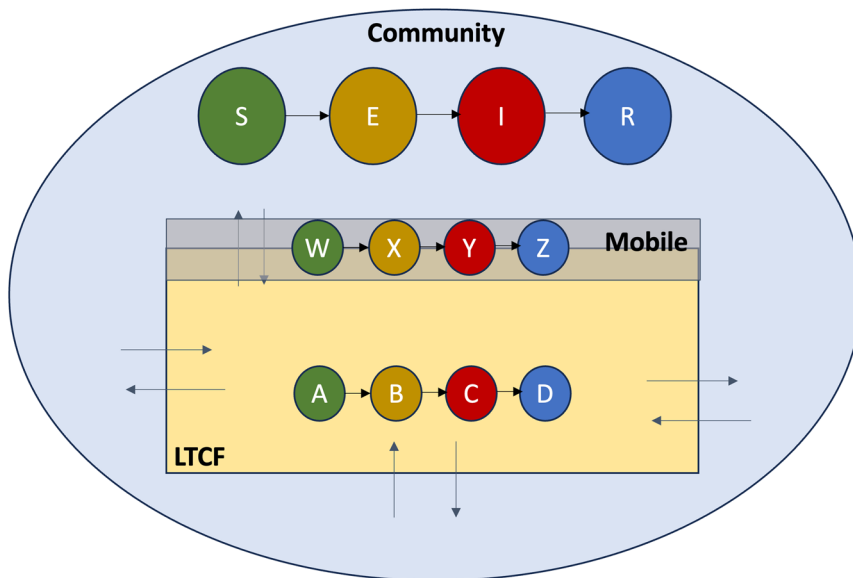


**Figure 1:** Model dynamics containing three sub-groups: non-mobile, mobile, and old-age home population.

**Table 1:** Definition of the population states

Variable	Definition
$S, E, I, R; Q$	Non-mobile population compartments
$W, X, Y, Z; T$	Mobile (to old-age homes) population compartments
$A, B, C, D; P$	Old-age home population compartments
$S, W, A$	Susceptible population compartments
$E, X, B$	Exposed population compartments (Infectious)
$I, Y, C$	Infected population compartments (Infectious)
$R, Z, D$	Recovered population compartments

Let  $\theta_1$ ,  $\theta_2$ , and  $\theta_3$  be the average number of contacts of Q, T, and P per unit time, respectively. Denoting NM to be the non-mobile community members, M-NV and M-V to be mobile community members that either do not visit or visit a LTCF, respectively, and LCO to be local senior residents from the LTCF, we can summarize their contacts via Table 2.

Let  $\tau$  denote the fraction of mobile youth that visit a LTCF and  $\omega = (1 - \tau)$  be the fraction of mobile youth that are in community. We can then describe the mixing patterns of individuals during the various interactions using appropriate mixing probabilities. We also assume that  $\gamma$  be the fraction of contacts that are reduced due to isolation in the LTCF. If individuals mix according to the proportional mixing scheme [9,11], then these mixing probabilities are defined and given as follows (Table 3):

- $\tilde{P}_{SX}$  is the mixing probability between non-mobile and mobile youth in the community;
- $\tilde{P}_{SE}$  is the mixing probability between non-mobile youth within their sub-group;
- $\tilde{P}_{WX}$  is the mixing probability between mobile youth within their sub-group;
- $\tilde{P}_{WE}$  is the mixing probability between mobile and non-mobile youth in the community;
- $\tilde{P}_{WC}$  is the mixing probability between the mobile youth that visit a LTCF and old-age members there;
- $\hat{P}_{AX}$  is the mixing probability between old-age members at the LTCF with the mobile youth from the community that visit them;
- $\hat{P}_{AB}$  is the mixing probability between old-age members at the LTCF with other **exposed** old-age members from the facility.
- $\hat{P}_{AC}$  is the mixing probability between old-age members at the LTCF with other **infected** old-age members from the facility.

Note that the mixing probabilities satisfy the following identities:

$$\begin{aligned}\tilde{P}_{SX} + \tilde{P}_{SE} &= 1, \\ \tilde{P}_{WX} + \tilde{P}_{WE} + \tilde{P}_{WC} &= 1, \\ \hat{P}_{AX} + \hat{P}_{AB} + \hat{P}_{AC} &= 1.\end{aligned}$$

Let  $f_Q$ ,  $f_T$ , and  $f_P$  be defined as the efficacy of the face mask worn by each sub-group and denote the proportion of people that uses face masks effectively. Also, let  $\bar{f}_i = 1 - f_i$  for  $i = Q, T, P$  denote the proportion that do not use face masks effectively. Note that  $f_P \gg f_Q$  and  $f_P \gg f_T$  as well as  $\theta_3 \ll \theta_1, \theta_3 \ll \theta_2$  assuming that

**Table 2:** Contact rates among the population

Group	Type of people contacted by	NM	Contacting who		
			M-NV	M-V	LCO
I	NM	$\theta_1$	$\theta_1$	0	0
II	M-NV	$\theta_2$	$\theta_2$	0	0
	M-V	0	0	$\theta_3$	$\theta_3$
III	LCO	0	0	$\theta_3$	$\theta_3$

**Table 3:** Definition of mixing probabilities

Mixing probability	Formula
$\tilde{P}_{SX} = \tilde{P}_b$	$\frac{\theta_2\omega T}{\theta_1Q + \theta_2\omega T}$
$\tilde{P}_{SE} = \tilde{P}_c$	$\frac{\theta_1Q}{\theta_1Q + \theta_2\omega T}$
$\bar{P}_{WX} = \bar{P}_b$	$\frac{\theta_2\omega T + \theta_2\tau T}{\theta_1Q + \theta_2\omega T + \theta_2\tau T + \theta_3P}$
$\bar{P}_{WE} = \bar{P}_c$	$\frac{\theta_1Q}{\theta_1Q + \theta_2\omega T + \theta_2\tau T + \theta_3P}$
$\bar{P}_{WC} = \bar{P}_d =$	$\frac{\theta_3P}{\theta_1Q + \theta_2\omega T + \theta_2\tau T + \theta_3P}$
$\hat{P}_{AX} = \hat{P}_b$	$\frac{\theta_2\tau T}{\theta_2\tau T + \theta_3P}$
$\hat{P}_{AB} = \hat{P}_c$	$\frac{\gamma\theta_3P}{\theta_2\tau T + \theta_3P}$
$\hat{P}_{AC} = \hat{P}_d$	$\frac{(1-\gamma)\theta_3P}{\theta_2\tau T + \theta_3P}$

the senior members in the LTCF will adhere to policies on face masks and social distancing much more than the youth. We also assume that old-age population does not have the ability to self-heal and disease-related death  $d_2$  is higher than the average mortality rate  $d_1$ .

The governing differential equations for the non-mobile population system can then be described by:

$$\frac{dS}{dt} = -\beta\theta_1\bar{f}_Q S \left[ \underbrace{\tilde{P}_c \frac{\bar{f}_Q E}{\omega T + Q}}_{\text{Non-Mobile; Non-Mobile}} + \underbrace{\tilde{P}_b \frac{\omega\bar{f}_T X}{\omega T + Q}}_{\text{Non-Mobile; Mobile}} \right], \quad (1)$$

$$\frac{dE}{dt} = \beta\theta_1\bar{f}_Q S \left[ \underbrace{\tilde{P}_c \frac{\bar{f}_Q E}{\omega T + Q}}_{\text{Non-Mobile; Non-Mobile}} + \underbrace{\tilde{P}_b \frac{\omega\bar{f}_T X}{\omega T + Q}}_{\text{Non-Mobile; Mobile}} \right] - \phi E, \quad (2)$$

$$\frac{dI}{dt} = \phi\rho E - aI - d_1 I, \quad (3)$$

$$\frac{dR}{dt} = \phi(1-\rho)E + aI. \quad (4)$$

The governing differential equations for the mobile (to old-age homes) population system can then be described by:

$$\frac{dW}{dt} = -\beta\theta_2\bar{f}_T W \left[ \underbrace{\bar{P}_b \frac{\omega^2\bar{f}_T X}{\omega T + Q}}_{\text{Mobile; Mobile}} + \underbrace{\bar{P}_c \frac{\omega\bar{f}_Q E}{\omega T + Q}}_{\text{Mobile; Non-mobile}} + \underbrace{\bar{P}_d \frac{\tau\bar{f}_P C}{\tau T + P}}_{\text{Mobile; Old-age}} \right], \quad (5)$$

$$\frac{dX}{dt} = \beta\theta_2\bar{f}_T W \left[ \underbrace{\bar{P}_b \frac{\omega^2\bar{f}_T X}{\omega T + Q}}_{\text{Mobile; Mobile}} + \underbrace{\bar{P}_c \frac{\omega\bar{f}_Q E}{\omega T + Q}}_{\text{Mobile; Non-mobile}} + \underbrace{\bar{P}_d \frac{\tau\bar{f}_P C}{\tau T + P}}_{\text{Mobile; Old-age}} \right] - \phi X, \quad (6)$$

$$\frac{dY}{dt} = \phi\rho X - aY - d_1 Y, \quad (7)$$

$$\frac{dZ}{dt} = \phi(1-\rho)X + aY. \quad (8)$$

The governing differential equations for the old-age home population system can then be described by:

$$\frac{dA}{dt} = -\beta\theta_3\bar{f}_PA \left[ \underbrace{\hat{P}_c \frac{\bar{f}_p B}{\tau T + P}}_{\text{Adults; Adults Exposed}} + \underbrace{\hat{P}_d \frac{\bar{f}_p C}{\tau T + P}}_{\text{Adults; Adults Infected}} + \underbrace{\hat{P}_b \frac{\tau \bar{f}_T X}{\tau T + P}}_{\text{Adults; Mobile}} \right], \quad (9)$$

$$\frac{dB}{dt} = \beta\theta_3\bar{f}_PA \left[ \underbrace{\hat{P}_c \frac{\bar{f}_p B}{\tau T + P}}_{\text{Adults; Adults Exposed}} + \underbrace{\hat{P}_d \frac{\bar{f}_p C}{\tau T + P}}_{\text{Adults; Adults Infected}} + \underbrace{\hat{P}_b \frac{\tau \bar{f}_T X}{\tau T + P}}_{\text{Adults; Mobile}} \right] - \phi B, \quad (10)$$

$$\frac{dC}{dt} = \phi B - \alpha C - d_2 C, \quad (11)$$

$$\frac{dD}{dt} = \alpha C. \quad (12)$$

In these model equations, the total population corresponding to the non-mobile youth is  $Q = S + E + I + R$ , corresponding to mobile youth, which is  $T = W + X + Y + Z$ , and corresponding to old-age members at the LTCF is  $P = A + B + C + D$ .

Parameters that are used and their definitions are given in Table 4.

**Table 4:** Parameter and variable description

Variable	Definition	Value
$\beta$	(Probability given a contact) effectiveness of successful transmission of infection	0.1 estimated
$\theta_1, \theta_2, \theta_3$	Number of contacts of an individual in a three categories (non-mobile (Q), mobile (T) and individuals in old-age home (P), respectively) of populations	0.48
$q$	Rate of self-isolation	( $1/q = 5$ days)
$l$	Proportion of individuals that rigorously isolate (effectiveness of isolation))	(0.5
$f_Q$	Efficacy of the face mask worn by population Q	0.5 varied
$f_T$	Efficacy of the face mask worn by population T	0.5 varied
$f_P$	Efficacy of the face mask worn by population P	0.8 varied
$1/\phi$	Average asymptomatic period	(6.4 days) [21]
$\rho$	Proportion of asymptomatic that self-heals	0.81
$1/\alpha$	Average symptomatic period	(7.6 days) (2–14) [14]
$d_1$	Average mortality rate	0.034 [14]
$d_2$		0.25
$\omega$	Fraction of mobile individuals that are in community	0.93 [20,24,25]
$\tau$	Fraction of mobile individuals that are in old-age homes and hence	0.07 [20,24,25]
$Q$	Non-mobile population	4,617 [20,24,25]
$T$	Mobile (to old-age homes) population	376 [25]
$P$	Old-age home population	480 [20,24,28]
$S(0)$		4,617
$E(0)$		0
$I(0)$		0
$R(0)$		0
$W(0)$		376
$X(0)$		0
$Y(0)$		0
$Z(0)$		0
$A(0)$		480
$B(0)$		1
$C(0)$		0
$D(0)$		0

### 3 Mathematical analysis

#### 3.1 Basic reproduction number

Reproductive number plays an important role in determining the dynamics of spread of a disease. We use here a general approach called the *next-generation matrix approach* [10,12,17] to find the basic reproduction number  $\mathcal{R}_0$ . Given that the infectious states:  $E$ ,  $X$ ,  $B$ ,  $I$ ,  $Y$ , and  $C$  in equations (1)–(12), we create a vector  $\mathcal{F}$  that represents the new infections flowing only into the exposed compartments given by:

$$\mathcal{F} = \{x_{11}E + x_{12}X, x_{21}X + x_{22}E + x_{23}C, x_{31}B + x_{32}C + x_{33}X, 0, 0, 0\}, \quad (13)$$

where

$$\begin{aligned} x_{11} &= (\beta\theta_1\bar{f}_Q Q)\tilde{P}_c \frac{\bar{f}_Q}{\omega T + Q}, \\ x_{12} &= (\beta\theta_1\bar{f}_Q Q)\tilde{P}_b \frac{\omega\bar{f}_T}{\omega T + Q}, \\ x_{21} &= (\beta\theta_2\bar{f}_T T)\bar{P}_b \frac{\omega^2\bar{f}_T}{\omega T + Q}, \\ x_{22} &= (\beta\theta_2\bar{f}_T T)\bar{P}_c \frac{\omega\bar{f}_Q}{\omega T + Q}, \\ x_{23} &= (\beta\theta_2\bar{f}_T T)\bar{P}_d \frac{\tau\bar{f}_P}{\tau T + P}, \\ x_{31} &= (\beta\theta_3\bar{f}_P P)\hat{P}_c \frac{\bar{f}_P}{\tau T + P}, \\ x_{32} &= (\beta\theta_3\bar{f}_P P)\hat{P}_d \frac{\bar{f}_P}{\tau T + P}, \\ x_{33} &= (\beta\theta_3\bar{f}_P P)\hat{P}_b \frac{\tau\bar{f}_T}{\tau T + P}. \end{aligned}$$

Along with  $\mathcal{F}$ , we also consider  $\mathcal{V}$ , which denotes the outflow from the infectious compartments in equations (1)–(12), which is given by:

$$\mathcal{V} = \{\phi E, \phi X, \phi B, \alpha_1 I - \rho\phi E, \alpha_1 Y - \rho\phi X, \alpha_2 C - \phi B\}, \quad (14)$$

where  $\alpha_i = \alpha + d_i$ ,  $i = 1, 2$ .

Next, we compute the Jacobian  $F$  from  $\mathcal{F}$  (see (6)), and the Jacobian  $V$  from  $\mathcal{V}$  (see (6)). Using matrices  $F$  and  $V$ , we compute the next-generation matrix  $FV^{-1}$ :

$$FV^{-1} = \begin{pmatrix} \frac{x_{11}}{\phi} & \frac{x_{12}}{\phi} & 0 & 0 & 0 & 0 \\ \frac{x_{22}}{\phi} & \frac{x_{21}}{\phi} & \frac{x_{23}}{a_2} & 0 & 0 & x_{23} \\ 0 & \frac{x_{33}}{\phi} & \left( \frac{x_{31}}{\phi} + \frac{x_{32}}{a_2} \right) & 0 & 0 & x_{32} \\ 0 & 0 & 0 & 0 & 0 & 0 \\ 0 & 0 & 0 & 0 & 0 & 0 \\ 0 & 0 & 0 & 0 & 0 & 0 \end{pmatrix}.$$

Note that  $(i, j)$  entry of the next-generation matrix  $FV^{-1}$  is the expected number of secondary infections in compartment  $i$  produced by individuals initially in compartment  $j$  assuming that the environment seen by the individual remains homogeneous for the duration of its infection. Also, matrix  $FV^{-1}$  is non-negative and therefore has a non-negative eigenvalue. The basic reproduction number can then be computed as

$\mathcal{R}_0 = \rho(FV^{-1})$ , which is the spectral radius of the matrix. This non-negative eigenvalue is associated with a non-negative eigenvector, which represents the distribution of infected individuals that produces the greatest number  $\mathcal{R}_0$  of secondary infections per generation. In order to calculate the eigenvalues of  $FV^{-1}$ , we consider the characteristic equation:

$$\det(FV^{-1} - \lambda I) = 0,$$

where  $\lambda$  denotes the eigenvalues of the matrix and  $I$  represents the identity matrix. This can be simplified to yield:

$$\det \begin{bmatrix} \frac{x_{11}}{\phi} - \lambda & \frac{x_{12}}{\phi} & 0 & 0 & 0 & 0 \\ \frac{x_{22}}{\phi} & \frac{x_{21}}{\phi} - \lambda & \frac{x_{23}}{a_2} & 0 & 0 & \frac{x_{23}}{a_2} \\ 0 & \frac{x_{33}}{\phi} & \left( \frac{x_{31}}{\phi} + \frac{x_{32}}{a_2} \right) - \lambda & 0 & 0 & \frac{x_{32}}{a_2} \\ 0 & 0 & 0 & -\lambda & 0 & 0 \\ 0 & 0 & 0 & 0 & -\lambda & 0 \\ 0 & 0 & 0 & 0 & 0 & -\lambda \end{bmatrix} = 0$$

The characteristic polynomial therefore is the following equation given by:

$$\lambda^3 + a_2\lambda^2 + a_1\lambda + a_0 = 0, \quad (15)$$

where

$$\begin{aligned} a_2 &= -\left( \frac{x_{11}}{\phi} + \frac{x_{21}}{\phi} + \frac{x_{31}}{\phi} + \frac{x_{32}}{a_2} \right), \\ a_1 &= \frac{x_{11}}{\phi} \cdot \frac{x_{21}}{\phi} + \left( \frac{x_{31}}{\phi} + \frac{x_{32}}{a_2} \right) \left( \frac{x_{11}}{\phi} + \frac{x_{22}}{\phi} \right) - \left( \frac{x_{23}}{a_2} \cdot \frac{x_{33}}{\phi} + \frac{x_{12}}{\phi} \cdot \frac{x_{22}}{\phi} \right), \\ a_0 &= \frac{x_{11}}{\phi} \cdot \frac{x_{23}}{a_2} \cdot \frac{x_{33}}{\phi} + \left( \frac{x_{31}}{\phi} + \frac{x_{32}}{a_2} \right) \cdot \left( \frac{x_{12}}{\phi} \cdot \frac{x_{22}}{a_2} - \frac{x_{11}}{\phi} \cdot \frac{x_{21}}{\phi} \right). \end{aligned}$$

The basic reproduction number  $\mathcal{R}_0$  corresponds to the dominant eigenvalue given by the dominant root of equation (15) given by:

$$\mathcal{R}_0 = -\frac{1}{3}a_2 + \sqrt[3]{R + \sqrt{M}} + \sqrt[3]{R - \sqrt{M}},$$

where

$$R = \frac{9a_2a_1 - 27a_0 - 2a_2^3}{54},$$

$$S = \frac{3a_1 - a_2^2}{9},$$

$$M = S^3 + R^2,$$

$$\det \begin{bmatrix} \hat{R}_{Q1} - \lambda & \hat{R}_{Q2} & 0 & \\ \hat{R}_{T1} & \hat{R}_{T2} - \lambda & \tilde{R}_T & \\ 0 & \hat{R}_{P1} & (\hat{R}_{P2} + \tilde{R}_P) - \lambda & \end{bmatrix} = 0,$$

where  $\hat{R}_* = \frac{*}{\phi}$  and  $\tilde{R}_* = \frac{*}{a_2}$   
where

$$\begin{aligned}\frac{x_{11}}{\phi} &= \widehat{R}_{Q1}, \\ \frac{x_{21}}{\phi} &= \widehat{R}_{Q2}, \\ \frac{x_{12}}{\phi} &= \widehat{R}_{T1}, \\ \frac{x_{22}}{\phi} &= \widehat{R}_{T2}, \\ \frac{x_{11}}{\phi} &= \widehat{R}_{P1}, \\ \frac{x_{21}}{\phi} &= \widehat{R}_{P1}.\end{aligned}$$

**Corollary 1.** If the adults in the long-term care are fully protected with face-masks ( $f_p = 1$ ), the infection dies out ( $\mathcal{R}_0 < 1$ ) if

where

$$\frac{x_{11}}{\phi} \cdot \frac{x_{21}}{\phi} + \frac{x_{12}}{\phi} \cdot \frac{x_{22}}{\phi} + \left( \frac{x_{11}}{\phi} + \frac{x_{21}}{\phi} \right) < 1. \quad (16)$$

**Corollary 2.** If the adults in the long-term care are fully protected with face-masks ( $f_p = 1$ ), the infection dies out ( $\mathcal{R}_0 < 1$ ) if

$$\widehat{R}_{Q1}\widehat{R}_{Q2} + \widehat{R}_{T1}\widehat{R}_{T2} + \widehat{R}_{P1}\widehat{R}_{P2} < 1,$$

**Corollary 3.** If the adults in the long-term care are fully protected with face-masks ( $f_p = 1$ ) as well as the mobile youth are fully protected with face-masks ( $f_T = 1$ ), then infection dies out ( $\mathcal{R}_0 < 1$ ) if

$$\frac{x_{11}}{\phi} < 1$$

Note that this suggests that

$$(\beta\theta_1\bar{f}_Q Q)\tilde{P}_c \frac{\bar{f}_Q}{\phi(\omega T + Q)} < 1,$$

or this yields a restriction on effective face mask efficacy for the non-mobile youth as follows:

$$f_Q > 1 - \sqrt{\frac{\phi(\omega T + Q)}{\beta\theta_1 Q \tilde{P}_c}}.$$

## 4 Computational experiments

### 4.1 Model implementation on CDC strategies

We consider here five scenarios given by CDC and implement in our model to understand the strategies that work in favor for LTCFs. We estimate the contact rate  $\theta$  based on the planning scenarios by CDC [14] as follows:

- **Scenario 1** [14]:

- Lower-bound values for virus transmissibility and disease severity
- Lower percentage of transmission prior to onset of symptoms
- Lower percentage of infections that never have symptoms and lower contribution of those cases to transmission

Using the expression of basic reproductive number  $R_0$  from [26], we estimate  $\theta$  to be 2.88.

- **Scenario 2** [14]:

- Lower-bound values for virus transmissibility and disease severity
- Higher percentage of transmission prior to the onset of symptoms
- Higher percentage of infections that never have symptoms and higher contribution of those cases to transmission

We estimate the contact rate  $\theta$  to be 3.17 based on the planning Scenario 2 by CDC [14] from [26].

- **Scenario 3** [14]:

- Upper-bound values for virus transmissibility and disease severity
- Lower percentage of transmission prior to onset of symptoms
- Lower percentage of infections that never have symptoms and lower contribution of those cases to transmission

We estimate the contact rate  $\theta$  to be 4.5 based on the planning Scenario 3 by CDC [14] from [26].

- **Scenario 4** [14]:

- Upper-bound values for virus transmissibility and disease severity
- Higher percentage of transmission prior to onset of symptoms
- Higher percentage of infections that never have symptoms and higher contribution of those cases to transmission

We estimate the contact rate  $\theta$  to be 4.89 based on the planning Scenario 4 by CDC [14].

- **Scenario 5** [14]:

- Parameter values for disease severity, viral transmissibility, and pre-symptomatic and asymptomatic disease transmission represent the best estimate, based on the latest surveillance data and scientific knowledge.

We estimate the contact rate  $\theta$  to be 3.43 based on the planning Scenario 5 by CDC [14].

For these five scenarios, the values of  $\theta_i$  for  $i = 1, 2, 3$  are calculated as follows:  $\theta_2 = 1.5 * \theta_1$  and  $\theta_3 = 0.5 * \theta_1$ . Note that this satisfies:  $\theta_3 < \theta_1 < \theta_2$ . The definition of CDC scenarios and the corresponding parameter estimates are collected in Tables 5 and 6, respectively.

The baseline case, defined to reflect early COVID-19 outbreak when interventions were yet to be initiated, is also considered in this analysis. The model parameter estimates for the baseline case were obtained from reference [26] and are collected in Table 6.

## 4.2 Numerical results

Using our model, we simulate the five scenarios given by CDC in Table 5 to understand and compare the dynamics of COVID-19 in LTCFs under different control strategies. We study the model for 30 days (to capture single outbreak burden) for the population of LTCF residents and visitors to the residents and non-visitors based on parameter estimates given in Table 6.

We divide the section into four subcases of the model describing different modeling assumptions on mixing and mortality. For each subcases, we simulate all the five scenarios. The cases are as follows:

Case 1: negligible disease mortality rate, proportional mixing population, and constant total population

Case 2: negligible disease mortality rate, heterogeneous mixing population, and constant total population

Case 3: high disease mortality rate and proportional mixing population

Case 4: high disease mortality rate, heterogeneous mixing population, and variable community population size.

We implement these sub-cases in the five CDC scenarios and compare the disease burden in each for a LTCF. The disease burden is defined by metrics such as the peak value of an outbreak; peak time of the outbreak, and

Table 5: Five planning CDC scenarios

CDC planning scenarios	Scenario 1	Scenario 2	Scenario 3	Scenario 4	Scenario 5
Lower-bound values for virus transmissibility and disease severity	Lower-bound values for virus transmissibility and disease severity	Upper-bound values for virus transmissibility and disease severity	Upper-bound values for virus transmissibility and disease severity	Upper-bound values for virus transmissibility and disease severity	Parameter values for disease severity, viral transmissibility, and pre-symptomatic and asymptomatic disease transmission that represent the best estimate, based on the latest surveillance data and scientific knowledge.
Lower percentage of transmission prior to onset of symptoms	Higher percentage of transmission prior to onset of symptoms	Lower percentage of transmission prior to onset of symptoms	Lower percentage of transmission prior to onset of symptoms	Higher percentage of transmission prior to onset of symptoms	
Lower percentage of infections that never have symptoms and lower contribution of those cases to transmission	Higher percentage of infections that never have symptoms and higher contribution of those cases to transmission	Higher percentage of infections that never have symptoms and lower contribution of those cases to transmission	Higher percentage of infections that never have symptoms and lower contribution of those cases to transmission	Higher percentage of infections that never have symptoms and higher contribution of those cases to transmission	

**Table 6:** Parameter values for different CDC scenarios

Parameters	Parameter values					
	Baseline	Scenario 1	Scenario 2	Scenario 3	Scenario 4	Scenario 5
$\theta$	5	2.88	3.17	4.5	4.89	3.43
$\theta_1$	5	2.88	3.17	4.5	4.89	3.43
$\theta_2$	5.42	4.32	4.76	6.75	7.34	5.15
$\theta_3$	4.58	1.44	1.56	2.25	2.45	1.72

**Table 7:** Proportional mixing Case 1 for five different CDC scenarios applied after 30 days in comparison with baseline (without deaths)

Parameters	Proportional mixing (without deaths)					
	Baseline	Scenario 1	Scenario 2	Scenario 3	Scenario 4	Scenario 5
$\mathcal{R}_0$ <b>Computed</b>	3.2969	2.6473	2.7205	3.0493	3.1448	2.7853
<b>Non-visitors</b>						
Peak value	0.1466	0.0008	0.0016	0.0993	0.1398	0.0074
Peak time	104	68	146	122	108	180
Epidemic size	0.6255	0.0066	0.0158	0.5106	0.6131	0.0426
<b>Visitors</b>						
Peak value	0.1119	0.0022	0.0026	0.0939	0.1329	0.0069
Peak time	105	47	51	123	108	180
Epidemic size	0.5200	0.0130	0.0227	0.4982	0.6009	0.0491
<b>LTCF members</b>						
Peak value	0.2101	0.0339	0.0330	0.0343	0.0350	0.0332
Peak time	68	31	30	35	46	30
Epidemic size	0.8118	0.0931	0.1017	0.2339	0.2997	0.11487

**Table 8:** Heterogeneous Case 2 for five different CDC scenarios applied after 30 days in comparison with baseline (without deaths)

Parameters	Heterogeneous mixing (without deaths)					
	Baseline	Scenario 1	Scenario 2	Scenario 3	Scenario 4	Scenario 5
$\mathcal{R}_0$ <b>Computed</b>	3.2969	2.6473	2.7205	3.0493	3.1448	2.7853
<b>Non-visitors</b>						
Peak value	0.4461	0.1373	0.1874	0.3791	0.4224	0.2304
Peak time	62	109	95	68	64	86
Epidemic size	0.9219	0.6079	0.6941	0.8825	0.9089	0.7502
<b>Visitors</b>						
Peak value	0.4287	0.1619	0.2175	0.4195	0.4636	0.2641
Peak time	62	107	94	66	63	85
Epidemic size	0.9067	0.7126	0.7935	0.9420	0.9587	0.8423
<b>LTCF members</b>						
Peak value	0.4077	0.3437	0.3439	0.3563	0.3571	0.3545
Peak time	36	30	30	31	31	31
Epidemic size	0.9198	0.6157	0.6337	0.7238	0.7456	0.6637

epidemic size of the non-visitors, visitors, and LTCF members for proportional and heterogeneous mixing population for 30 days in comparison with baseline scenario (Tables 7, 8, 9, and 10 collect results).

The dynamics of the non-visitors, visitors, and LTCF members for the five CDC scenarios applied after 30 days compared with baseline are shown for proportional mixing without deaths (Figure 2, i.e., Case 1),

**Table 9:** Proportional mixing Case 3 for five different CDC scenarios applied after 30 days in comparison with baseline (with deaths)

Proportional mixing (with deaths)						
Parameters	Baseline	Scenario 1	Scenario 2	Scenario 3	Scenario 4	Scenario 5
$\mathcal{R}_0$ Computed	3.2969	2.6473	2.7205	3.0493	3.1448	2.7853
<b>Non-visitors</b>						
Peak value	0.1325	0.0002	0.0003	0.0908	0.1290	0.00204
Peak time	121	44	180	143	123	180
Epidemic size	0.5323	0.0013	0.0032	0.4021	0.5225	0.0093
Deaths	0.0788	0.0002	0.0005	0.0591	0.0774	0.0014
<b>Visitors</b>						
Peak value	0.1010	0.0004	0.0004	0.0862	0.1230	0.0018
Peak time	122	37	40	144	124	180
Epidemic size	0.4158	0.0018	0.0037	0.3824	0.5007	0.0094
Deaths	0.0616	0.0003	0.0005	0.0562	0.0741	0.0014
<b>LTCF members</b>						
Peak value	0.0429	0.0083	0.0085	0.0086	0.0087	0.00855
Peak time	104	30	31	31	31	31
Epidemic size	0.1584	0.0095	0.0100	0.0199	0.0267	0.0105
Deaths	0.3010	0.0180	0.0191	0.0379	0.0507	0.0199

**Table 10:** Heterogeneous mixing Case 4 for five different CDC scenarios applied after 30 days in comparison with baseline (with deaths)

Heterogeneous mixing (with deaths)						
Parameters	Baseline	Scenario 1	Scenario 2	Scenario 3	Scenario 4	Scenario 5
$\mathcal{R}_0$ computed	3.2969	2.6473	2.7205	3.0493	3.1448	2.7853
<b>Non-visitors</b>						
Peak value	0.4283	0.1281	0.1758	0.3621	0.4048	0.2170
Peak time	64	114	100	70	66	91
Epidemic size	0.8027	0.5271	0.6039	0.7684	0.7914	0.65313
Deaths	0.1192	0.0782	0.0897	0.1141	0.1175	0.0970
<b>Visitors</b>						
Peak value	0.4133	0.1519	0.2052	0.4030	0.4468	0.25028
Peak time	64	112	98	69	65	89
Epidemic size	0.7883	0.6170	0.6895	0.8197	0.8344	0.7324
Deaths	0.1171	0.0915	0.1024	0.1218	0.1239	0.1088
<b>LTCF members</b>						
Peak value	0.2547	0.2159	0.2139	0.2124	0.2136	0.2118
Peak time	36	31	30	30	31	30
Epidemic size	0.2934	0.1673	0.1708	0.1959	0.2052	0.17425
Deaths	0.5575	0.3179	0.3244	0.3723	0.3899	0.3310

heterogeneous mixing without deaths (Figure 3, i.e., Case 2), proportional mixing with deaths (Figure 4, i.e., Case 3), and heterogeneous mixing with deaths (Figure 5, i.e., Case 4).

We observe that heterogeneous mixing population makes epidemic worse as compared to epidemic size in homogeneous mixing population. Moreover, in the heterogeneous mixing population, the epidemic burden is about 100 times more for community members (visitors and non-visitors) than for the LTCF population. That is, under heterogeneous mixing situation, which may occur due to continuous changes in the population behaviors, can create worse epidemic and particularly for long term care residents, with respect to metrics considered in this study.

Strategies 1, 2, and 5 result in almost similar burden and are the best followed by Strategy 3, whereas Strategy 4 is the worst among all the strategies. This statement is true for both homogeneous and

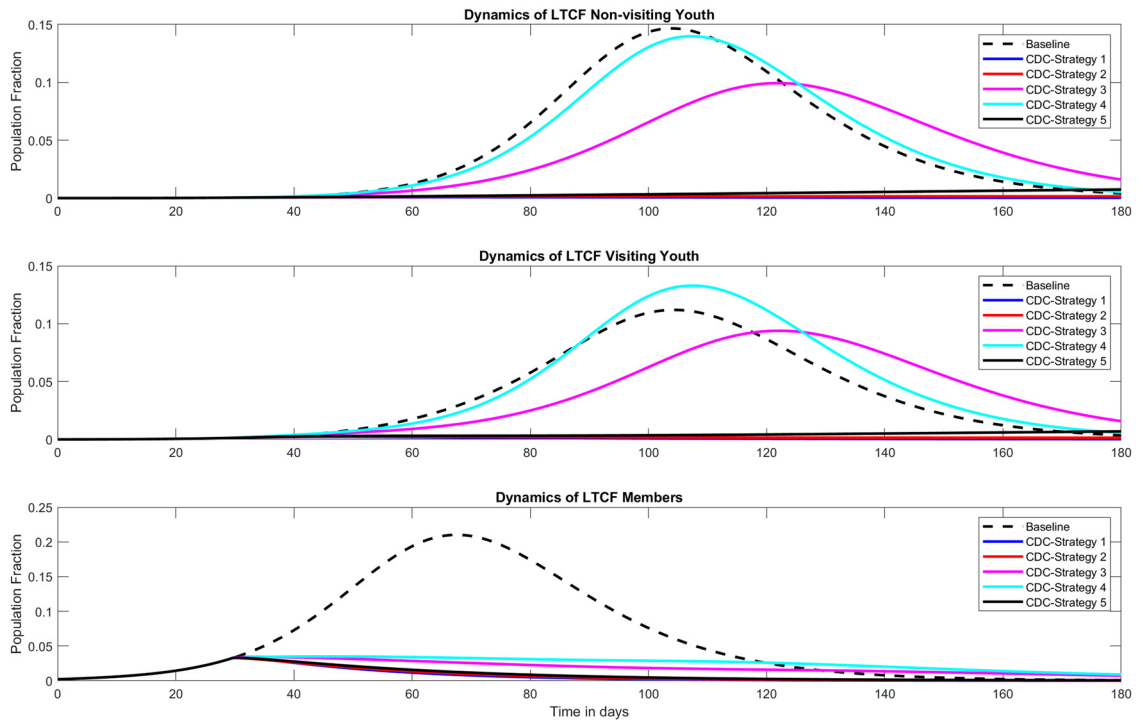


**Figure 2:** Dynamics of the non-visitors, visitors, and LTCF members for five CDC scenarios applied after 30 days compared with baseline for proportional mixing without deaths.

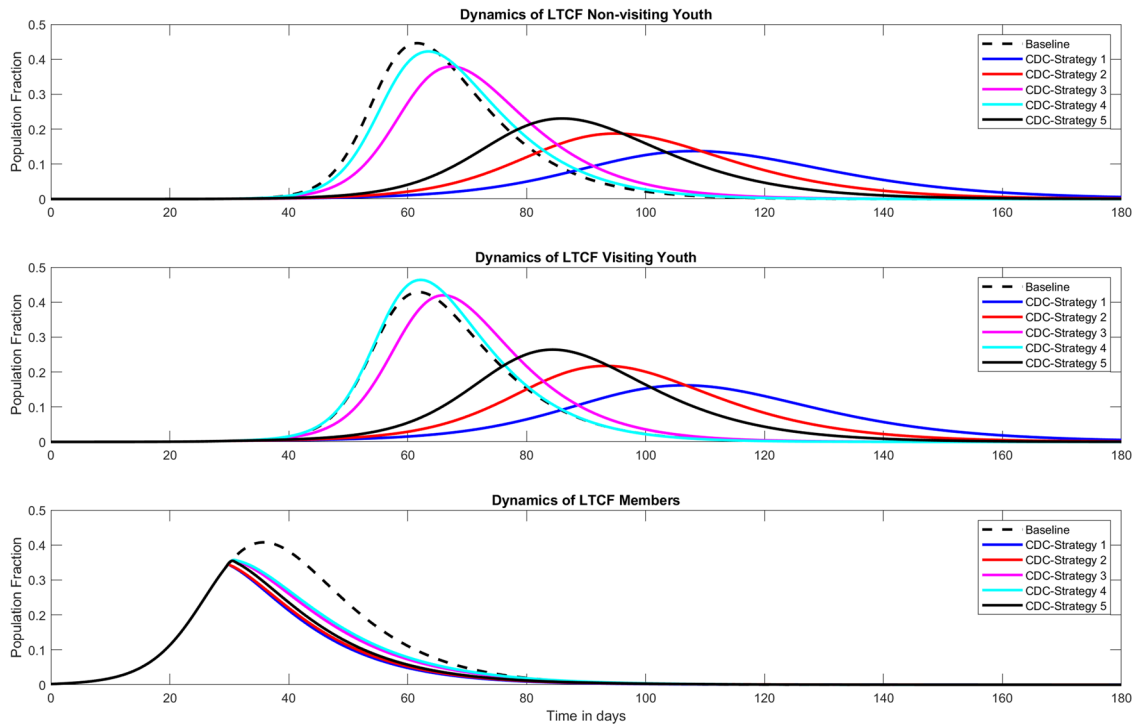


**Figure 3:** Dynamics of the non-visitors, visitors, and LTCF members for five CDC scenarios applied after 30 days compared with baseline for heterogeneous mixing without deaths.

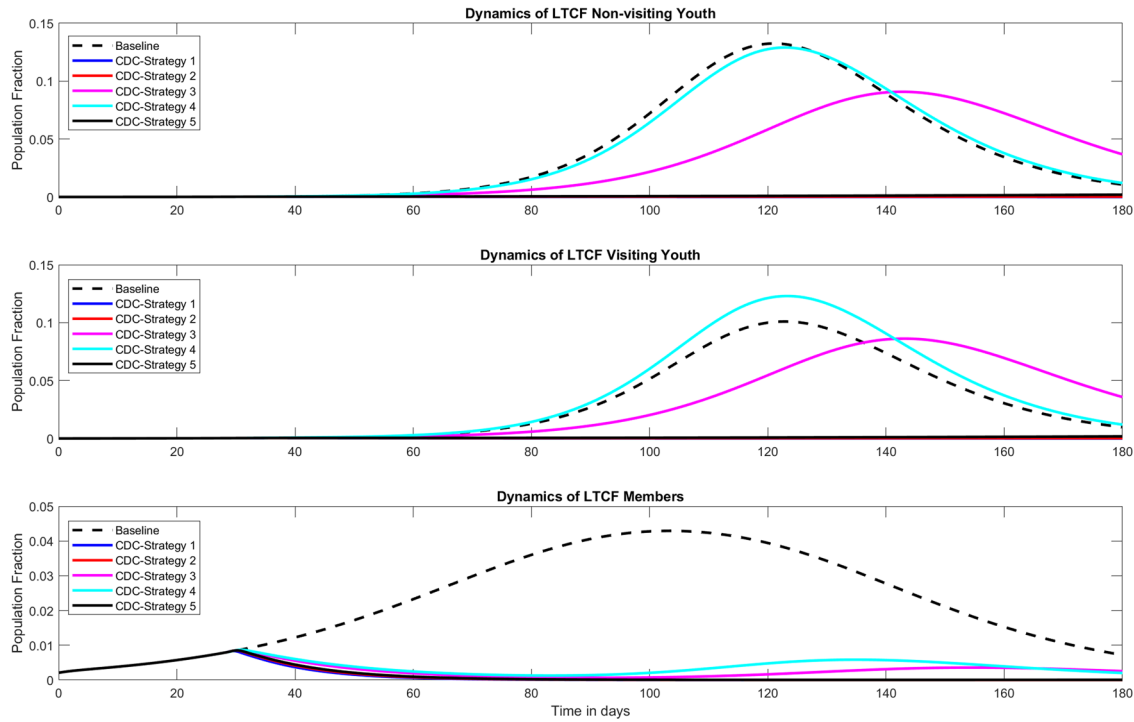


**Figure 4:** Dynamics of the non-visitors, visitors, and LTCF members for five CDC scenarios applied after 30 days compared with baseline for proportional mixing with deaths.

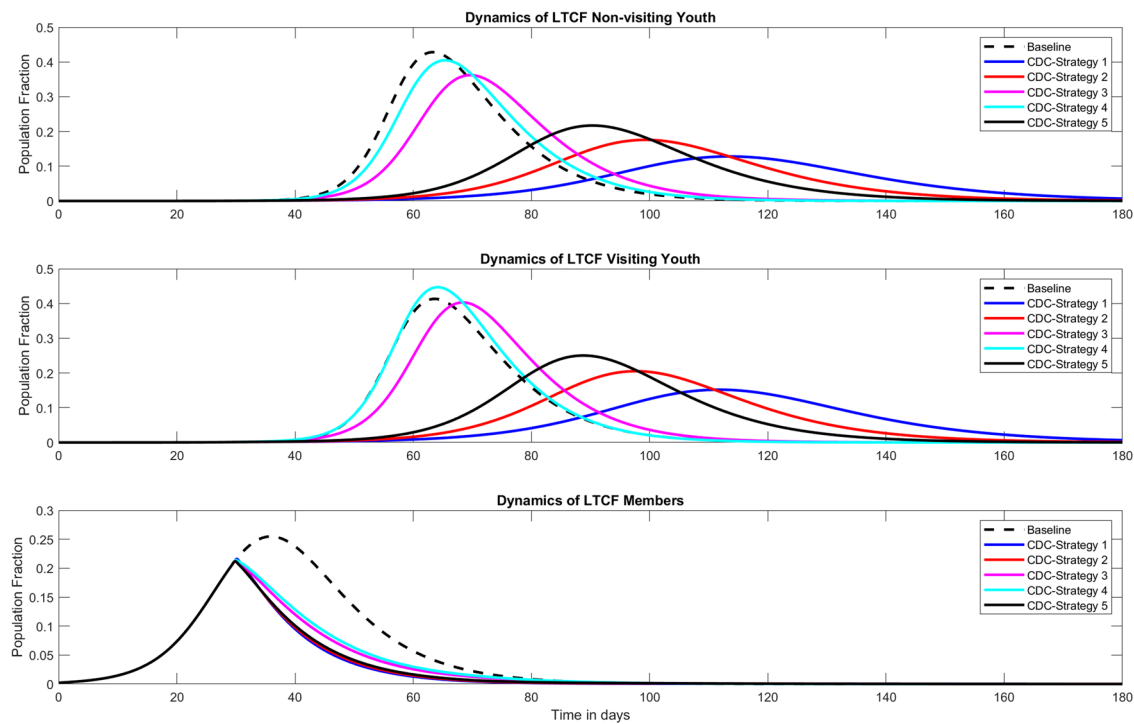


**Figure 5:** Dynamics of the non-visitors, visitors, and LTCF members for five CDC scenarios applied after 30 days compared with baseline for heterogeneous mixing with deaths.

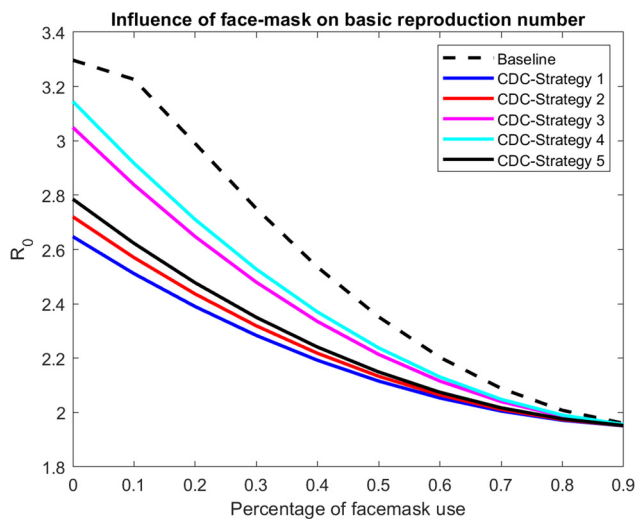


**Figure 6:** Influence of face mask on  $R_0$  for five CDC scenarios applied after 30 days compared with baseline.

heterogeneous mixing population. Figure 6 shows the influence of face masks on  $R_0$  for the five CDC scenarios applied after 30 days compared with baseline simulation. Strategy 1 has the lowest estimated  $R_0$  followed by Strategies 2, 3, 5, and 4. That is, 30-day disease burden is low in the Scenarios 1, 2, and 5 when compared with Scenarios 3 and 4. This is because transmission rate and/or disease severity rate are at lower levels in case of Scenarios 1, 2, and 5. The lower transmission rate results in slower spread of infection in the population, whereas lower disease severity rate results in shorter infectious period. The epidemic occurs faster with high peak in Scenario 4 (followed by Scenario 3) as compared with other scenarios. This is the result of higher estimated rate of reproduction number in these two scenarios.

## 5 Discussion

The role of LTCFs population is important for understanding outbreak of COVID-19 in the community. This is because the rate of spread could be high in LTCF as it consists of vulnerable adults with pre-existing health conditions and compromised immune system. The infectious disease model capturing mixing strategies of populations interacting with residents is thus one of the powerful methods to quickly understand the dynamics of disease spread.

We consider here two types of social contexts (community and LTCFs) and three different groups of interacting populations (non-mobile individuals in the community who do not visit LTCFs, mobile individuals in the community who visit LTCFs, and residents of LTCFs). We use a susceptible-exposed-infectious-recovered-type model within each sub-group and define mixing probabilities to understand the strategies that would work well in these facilities for five different CDC planning scenarios. Here, we aim to identify and quantify the roles of different subpopulations (residents, visitors, non-visitors) and the mixing strategies associated with them to better control COVID-19 in these facilities.

Our results suggest that heterogeneous mixing worsens the epidemic as compared to homogeneous mixing: the epidemic burden is hundreds of times greater for community spread (between visitors and non-visitors) than within the facility population. In both mixing scenarios, CDC Strategies 1, 2, and 5 have similarly best outcomes, followed by Strategies 3 and 4 is the worst approach. We also studied the influence of face mask on  $R_0$  for five CDC scenarios and found that Strategy 1 has the lowest reproductive number.

Due to the lack of comprehensive data, the study considered only aggregated estimates from multiple unrelated studies. However, the impact of parameter estimates on the results captured uncertainty associated

with key model parameters. Limited epidemiological scenarios were considered that capture situations in the United States only.

In the future, we would like to exercise this model with more data-extensive work that will incorporate explicit human behaviors through mixing empirical studies. Extension of the model can be considered that will require epidemiological states such as states consisting of individuals who are vaccinated and/or under other interventions.

**Acknowledgments:** We certify that the submission is original work and is not under review at any other publication.

**Funding information:** All co-authors have seen and agree with the contents of the manuscript, and there is no financial interest to report.

**Author contributions:** All authors contributed equally to this work.

**Conflict of interest:** The authors have no conflicts of interest to declare.

## References

- [1] Ajbar, A., Alqahtani, R. T., & Boumaza, M. (2021). Dynamics of an SIR-based COVID-19 model with linear incidence rate, nonlinear removal rate, and public awareness. *Frontiers in Physics*, 9, 13. doi: 10.3389/fphy.2021.634251.
- [2] Akman, O., Chauhan, S., Ghosh, A., Liesman, S., Michael, E., Mubayi, A., ..., Tripathi, J. P. (2022). The hard lessons and shifting modeling trends of COVID-19 dynamics: Multiresolution modeling approach. *Bulletin of Mathematical Biology*, 84, 1–30.
- [3] Brauer, F. (1990). Models for the spread of universally fatal diseases. *Journal of Mathematical Biology*, 28(4), 451–462.
- [4] Brauer, F. (2005). The Kermack-McKendrick epidemic model revisited. *Mathematical Biosciences*, 198(2), 119–131.
- [5] Brauer, F. (2006). Some simple epidemic models. *Mathematical Biosciences & Engineering*, 3(1), 1.
- [6] Brauer, F. (2008). Age-of-infection and the final size relation. *Mathematical Biosciences & Engineering*, 5(4), 681.
- [7] Brauer, F., Castillo-Chavez, C., & Castillo-Chavez, C. (2012). *Mathematical models in population biology and epidemiology* (Vol. 2, p. 508). New York: Springer.
- [8] Brauer, F., Castillo-Chavez, C., & Feng, Z. (2019). *Mathematical models in epidemiology* (Vol. 32). New York: Springer.
- [9] Busenberg, S., & Castillo-Chavez, C. (1991). A general solution of the problem of mixing of subpopulations and its application to risk- and age-structured epidemic models for the spread of AIDS. *Mathematical Medicine and Biology: A Journal of the IMA*, 8(1), 1–29.
- [10] Castillo-Chavez, C., Cooke, K., Huang, W., & Levin, S. A. (1989). The role of long periods of infectiousness in the dynamics of acquired immunodeficiency syndrome (AIDS). In: *Mathematical Approaches to Problems in Resource Management and Epidemiology* (pp. 177–189). Berlin, Heidelberg: Springer.
- [11] Castillo-Chavez, C., Song, B., & Zhang, J. (2003). An epidemic model with virtual mass transportation: The case of smallpox in a large city. In: *Bioterrorism: Mathematical Modeling Applications in Homeland Security* (pp. 173–197). Society for Industrial and Applied Mathematics. Germany: Springer International Publishing Berlin.
- [12] Castillo-Chavez, C., Velasco-Hernandez, J. X., & Friedman, S. (1994). Modeling contact structures in biology. In *Frontiers in Mathematical Biology* (pp. 454–491). Berlin, Heidelberg: Springer.
- [13] CDC COVID-19 Response Team, CDC COVID-19 Response Team, CDC COVID-19 Response Team, Bialek, S., Boundy, E., Bowen, V., Chow, N., Cohn, A., Dowling, N., ..., Gierke, R. (2020). Severe outcomes among patients with coronavirus disease 2019 (COVID-19)–United States, February 12–March 16, 2020. *Morbidity and Mortality Weekly Report*, 69(12), 343–346.
- [14] COVID-19 Pandemic Planning Scenarios, Uniform Resource Locator: <https://www.cdc.gov/coronavirus/2019-ncov/hcp/planning-scenarios.html>. 2021.
- [15] Chidambaram P. (2020). <https://www.kff.org/coronavirus-covid-19/issue-brief/state-reporting-of-cases-and-deaths-due-to-covid-19-in-long-term-care-facilities/>.
- [16] Comas-Herrera, A., Zalakaín, J., Lemmon, E., Henderson, D., Litwin, C., Hsu, A. T., ..., Fernández, J. L. (2020). *Mortality associated with COVID-19 in care homes: International evidence*. Article in LTCcovid.org, International Long-term Care Policy Network, CPEC-LSE, 14.
- [17] Diekmann, O., Heesterbeek, J. A. P., & Metz, J. A. (1990). On the definition and the computation of the basic reproduction ratio  $R_0$  in models for infectious diseases in heterogeneous populations. *Journal of Mathematical Biology*, 28(4), 365–382.
- [18] Dora, A. V., Winnett, A., Jatt, L. P., Davar, K., Watanabe, M., Sohn, L., ..., Goetz, M. B., (2020). Universal and serial laboratory testing for SARS-CoV-2 at a long-term care skilled nursing facility for veterans–?Los Angeles, California, 2020. *Morbidity and Mortality Weekly Report*, 69(21), 651.

- [19] Kimball, A., Hatfield, K. M., Arons, M., James, A., Taylor, J., Spicer, K., ..., Bell, J. M. (2020). Asymptomatic and presymptomatic SARS-CoV-2 infections in residents of a long-term care skilled nursing facility—King County, Washington, March 2020. *Morbidity and Mortality Weekly Report*, 69(13), 377.
- [20] King County, Update: King County COVID-19 case numbers for March 6, 2020, kingcounty.gov, 2020.
- [21] Lauer, S. A., Grantz, K. H., Bi, Q., Jones, F. K., Zheng, Q., Meredith, H. R., ..., Lessler, J. (2020). The incubation period of coronavirus disease 2019 (COVID-19) from publicly reported confirmed cases: Estimation and application. *Annals of Internal Medicine*, 172(9), 577–582.
- [22] McMichael, T. M., Currie, D. W., Clark, S., Pogosjans, S., Kay, M., Schwartz, N. G., ..., Ferro, J. (2020). Epidemiology of COVID-19 in a long-term care facility in King County, Washington. *New England Journal of Medicine*, 382(21), 2005–2011.
- [23] Nuño, M., Reichert, T. A., Chowell, G., & Gumel, A. B. (2008). Protecting residential care facilities from pandemic influenza. *Proceedings of the National Academy of Sciences*, 105(30), 10625–10630.
- [24] Pare, M. (2020). *Five coronavirus deaths at Washington facility belonging to Cleveland, Tennessee, company*. <https://www.timesfreepress.com/news/2020/mar/02/cleveland-tennessee-based-life-care-centers-america/>.
- [25] Population of South Juanita, Kirkland, Washington, Statisticalatlas.com/neighborhood/Washington/Kirkland/South-Juanita/Population, Statistical Atlas, 2020.
- [26] Rojas, J. H., Paredes, M., Banerjee, M., Akman, O., & Mubayi, A. (2022). Mathematical modeling and dynamics of SARS-CoV-2 in Colombia. *Letters in Biomathematics*, 9(1), 41–56.
- [27] Saade, M., Ghosh, S., Banerjee, M., & Volpert, V. (2023). An epidemic model with time delays determined by the infectivity and disease durations. *Mathematical Biosciences and Engineering*, 20(7), 12864–12888.
- [28] Sacchetti, M., Nguyen, A., & Kirkland, W. (2020). *Becomes epicenter of coronavirus response as cases spread*. Washington Post.
- [29] Worldometer, D. (2020). *COVID-19 coronavirus pandemic*. World Health Organization. [www.worldometers.info](http://www.worldometers.info).
- [30] Yourish, K., Rebecca Lai, K. K., Ivory, D., & Smith, M. (2020). *Home residents or workers*. The New York Times.

## Appendix

We compute the Jacobian  $F$  from  $\mathcal{F}$  given by:

$$F = \begin{pmatrix} x_{11} & x_{12} & 0 & 0 & 0 & 0 \\ x_{22} & x_{21} & 0 & 0 & 0 & x_{23} \\ 0 & x_{33} & x_{31} & 0 & 0 & x_{32} \\ 0 & 0 & 0 & 0 & 0 & 0 \\ 0 & 0 & 0 & 0 & 0 & 0 \\ 0 & 0 & 0 & 0 & 0 & 0 \end{pmatrix},$$

and the Jacobian  $V$  from  $\mathcal{V}$  given by:

$$V = \begin{pmatrix} \phi & 0 & 0 & 0 & 0 & 0 \\ 0 & \phi & 0 & 0 & 0 & 0 \\ 0 & 0 & \phi & 0 & 0 & 0 \\ -\rho\phi & 0 & 0 & a_1 & 0 & 0 \\ 0 & -\rho\phi & 0 & 0 & a_1 & 0 \\ 0 & 0 & -\phi & 0 & 0 & a_2 \end{pmatrix}$$

Using matrices  $F$  and  $V$ , one can then compute the next-generation matrix  $FV^{-1}$  to be:

$$FV^{-1} = \begin{pmatrix} \frac{x_{11}}{\phi} & \frac{x_{12}}{\phi} & 0 & 0 & 0 & 0 \\ \frac{x_{22}}{\phi} & \frac{x_{21}}{\phi} & \frac{x_{23}}{a_2} & 0 & 0 & \frac{x_{23}}{a_2} \\ 0 & \frac{x_{33}}{\phi} & \left( \frac{x_{31}}{\phi} + \frac{x_{32}}{a_2} \right) & 0 & 0 & \frac{x_{32}}{a_2} \\ 0 & 0 & 0 & 0 & 0 & 0 \\ 0 & 0 & 0 & 0 & 0 & 0 \\ 0 & 0 & 0 & 0 & 0 & 0 \end{pmatrix}.$$